Target Morphologies via a Two-Step Dissolution-Quench Process in Polymer Blends

Nigel Clarke*

Department of Chemistry, University of Durham, Durham, DH1 3LE, United Kingdom

(Received 22 October 2001; published 31 October 2002)

A novel process for obtaining controlled morphologies in polymer blends is modeled numerically. Particles of one type of polymer are allowed to dissolve in a matrix of a dissimilar polymer. Prior to complete dissolution the blend is quenched into the two-phase region, such that phase separation takes place. The combination of the incomplete dissolution and the wavelength selection process associated with phase separation results in particles that during the "intermediate" stages have a core that is significantly richer in the matrix material.

DOI: 10.1103/PhysRevLett.89.215506 PACS numbers: 61.41.+e, 64.75.+g

There has recently been great interest in targeted morphologies in polymer blends, block copolymers, and polymer films. The ability to produce materials with a specified morphology is highly desirable since the final mesoscale structure determines many of the properties of the material. Polymer blends with cocontinuous and droplet structures, and block copolymers that exhibit a wide variety of equilibrium and nonequilibrium morphologies, have long been exploited for their enhanced mechanical properties. More recently the use of two-phase blends and copolymers has attracted attention for photonic [1] and other electronic applications [2,3]. Block copolymers have particular appeal since the morphology can be controlled by varying the ratio of the block lengths and/or the architecture. Naturally, the length scale associated with the microstructure is dictated by the size of the polymer blocks. Although not impossible, it is nontrivial and costly to produce copolymers with lengths commensurate with the wavelength of light, a requirement if such polymers are to be used in photonic applications. Blends, on the other hand, can phase separate with a wide range of length scales ranging from tens of nanometers to hundreds of microns.

Phase separation occurs when a polymer blend is "quenched" from the one-phase region to the two-phase region of its phase diagram. The dynamics of phase separation, and hence the transient structures, depend on whether the blend is quenched into the metastable or the unstable state. In the former case, phase separation proceeds by nucleation and growth, resulting in droplet-like structures. In the latter, the blend phase separates spontaneously into a cocontinuous structure with a preferred length scale dominating, a process known as spinodal decomposition.

A more controlled approach to phase separation in blends was first explored by studying surface-directed spinodal decomposition [4]. Proceeding from this work, a considerable effort has been devoted to the study of phase separation in confined geometries [5]. Of particular potential is the use of patterned substrates to influence blend morphology and to produce anisotropic phase separated structures in thin films [6–8]. Another possibility is to influence the morphology by dissolving filler particles in a blend [9,10].

In this Letter, we consider a simple, controllable method for producing unusual morphologies. The method is similar to the concept of a two step quench process, studied experimentally [11–13]. In our model we start with undissolved particles dispersed in a matrix, with the bulk composition being such that the blend is miscible. During dissolution the interface between the particle and the matrix broadens with time and eventually disappears. If the blend is then quenched into the unstable region, phase separation occurs, but will be greatly affected by the presence of the inhomogeneities.

We model the kinetics of this process using the theory developed by Cahn and Hilliard [14]. In order to emphasize the underlying phenomena we consider only symmetric blends, in which the two components have the same degree of polymerization, N. For simplicity we neglect hydrodynamic effects, noting that, while these will play an important role in the very late stages of coarsening, the development of the transient morphologies should not be significantly affected. The starting point is the continuity equation: the rate of change of concentration in a given volume element is equal to the divergence of the flux of material into the element. The flux is then assumed to be proportional to the gradient of the chemical potential difference between the two components. The Cahn-Hilliard model was modified by Cook [15] to include the effects of thermal noise, and later modified for polymeric systems [16–18]. The simplest version appropriate to symmetric polymer blends is [19]

$$\frac{\partial \phi(\mathbf{r}, t)}{\partial t} = \nabla \cdot D\phi(1 - \phi)\nabla\left(\frac{\delta F_{\mathrm{mix}}\{\phi(\mathbf{r}, t)\}}{\delta \phi}\right) + \xi(\mathbf{r}, t), \tag{1}$$

where $\phi(\mathbf{r}, t)$ is the local volume fraction of component A, $F_{\mathrm{mix}}\{\phi(\mathbf{r}, t)\}$ is the free energy of mixing, and $\xi(\mathbf{r}, t)$ is the thermal noise. Incompressibility is assumed, such that $\phi_B(\mathbf{r}, t) = 1 - \phi(\mathbf{r}, t)$, where $\phi_B(\mathbf{r}, t)$ is the local volume

fraction of component B. We will assume that D, the self-diffusion coefficient, is a constant. We further assume that the free energy for the mixture is given by the Flory-Huggins theory [20] modified to account for the energetic costs of gradients in the concentration,

$$\frac{F_{\mathrm{mix}}}{k_B T} = \int_V d\mathbf{r}\left[\frac{1}{N}\{\phi \ln\phi + (1-\phi)\ln(1-\phi)\} + \chi\phi(1-\phi) + \kappa|\nabla\phi|^2 \right], \tag{2}$$

where χ is the Flory-Huggins dimensionless interaction parameter and the integral is performed over the volume, V, of the sample. The spinodal curve, the boundary between the metastable and the unstable regions, is given by $\chi_s = 1/2\phi(1-\phi)$, and the interfacial energy [16] by $\kappa = b^2/36\phi(1-\phi)$, where b is the length of a statistical repeat unit within a polymer. By combining Eqs. (1) and (2) and rescaling into a dimensionless form, we arrive at

$$\frac{\partial\phi(\mathbf{r},\tau)}{\partial\tau} = \nabla\cdot\phi(1-\phi)\nabla\left[\frac{1}{N|\chi-\chi_s|}\ln\frac{\phi}{1-\phi} - \frac{2\chi\phi}{|\chi-\chi_s|} + \frac{1-2\phi}{36\phi^2(1-\phi)^2}(\nabla\phi)^2 - \frac{1}{18\phi(1-\phi)}\nabla^2\phi\right], \tag{3}$$

where $\tau = ND(\chi-\chi_s)^2 t/b^2$, $\mathbf{x} = \sqrt{|\chi-\chi_s|}\mathbf{r}/b$, and the noise term has been neglected. It is straightforward to numerically solve Eq. (3) by the finite difference method; details are given in Ref. [19]. The inclusion of the noise term greatly increases the computation time and is believed not to affect the general behavior. However, noise is necessary for the phase separation to occur following a quench into the two-phase region, since the above equations will not evolve from a truly homogenous mixture. It is standard practice to generate these variations by adding a small random fluctuation in volume fraction to each lattice site at the start of a simulation only. Such an approach has been shown to reproduce many of the features associated with phase separation in polymer blends [19].

We have solved Eq. (3) for a mixture of circular particles of one component in a matrix of the other component. We work in two dimensions, using periodic boundary conditions. The logarithmic terms in the free energy give rise to numerical instabilities if the concentration of the matrix is $\phi_B = 0$ and that of the particles is $\phi_B = 1$, so we choose a matrix with $\phi_B = 0.05$ and particles with $\phi_B = 0.95$. Also to improve stability, we smooth the boundary between particles and matrix by setting the concentration at any point on the discretized grid to be the average over that of immediate nearest neighbors. Such stability problems should be improved by the use of more sophisticated numerical schemes (such as the finite element method). The particles are placed at random on the grid, such that no particles overlap. The effects of interparticle correlations are not considered in this Letter, but may have interesting consequences, particularly if the length scale of phase separation is similar to that of interparticle spacing.

The dissolution process corresponds to $\chi < \chi s$, so that the blend is in the one-phase region. During dissolution the blend is quenched into the two-phase region; i.e., we apply a step change in χ, so that $\chi > \chi s$. Because of the scaling, the conversion from the dimensionless spatial variable to real space is determined by $|\chi - \chi s|$. In order to simplify the numerical procedure, and to avoid having to rescale the lattice, we choose $|\chi - \chi s|$ to be the same before and after the quench. When the quench is applied, the volume fraction at each point on the grid is modified by a small random amount ($\pm$ 0.0005), to mimic the thermal noise. Figure 1 shows a series of snapshots from

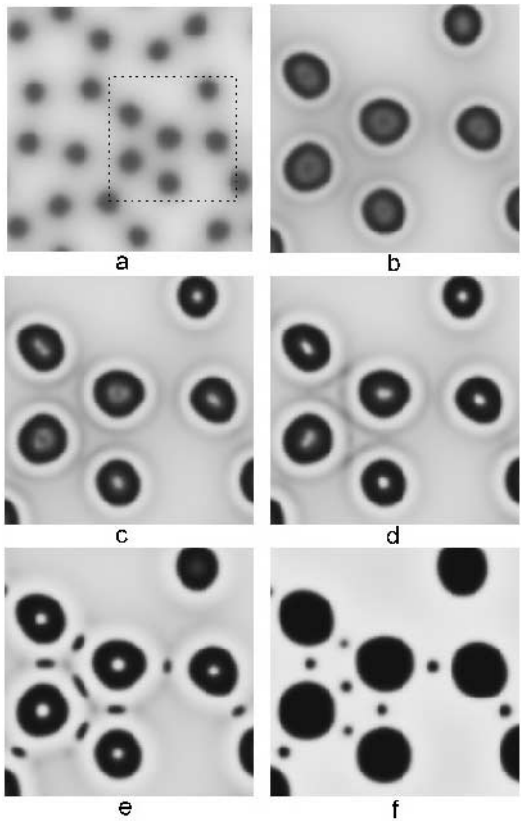

FIG. 1. Development of the morphology following the quench into the spinodal region ($R = 16$). Time steps, $\tau/\Delta\tau$, after the quench: (a) 10, (b) 500, (c) 794, (d) 1000, (e) 2000, and (f) 10 000. To highlight the existence of cores rich in component A, only a selected 128^2 area of the simulation, corresponding to the boxed region in (a) is shown in (b) to (f). The grey scale range, which is the same for all snapshots, is such that white represents regions of pure A, and black represents regions of pure B.

a solution of 21 particles of component B each of radius $R = 16$ lattice steps placed on a 256^2 grid, so that the volume fraction of B is $\phi_B \approx 0.29$. The spatial and temporal steps were $\Delta x = 0.25$ and $\Delta\tau = 0.002$, respectively. Different step sizes were also studied to ensure that the results were not an artifact of the discretization. N was chosen to be 200; hence, the spinodal corresponds to $\chi_s = 0.0121$, and we choose $|\chi - \chi s| = 0.000\,24$. From the scaling parameters the radius of the particles is $\sim 250b$, and b is typically of the order of angstroms. Immediately after the quench, applied when $\tau/\Delta\tau = 6000$, it is clear that the particles are not fully dissolved. During the phase separation, the wavelength selection process associated with spinodal decomposition leads to a core rich in component A developing within a shell of component B; it can be seen that the difference in volume fraction between the two becomes quite significant. For such a core to develop it is essential that the size of the particle is larger than the initial preferred wavelength of phase separation, λ_m, determined by linearizing Eq. (3) for small fluctuations, from which it can be shown that $\lambda_m \approx 2\pi/\sqrt{18\phi(1-\phi)}$, i.e., $2R/\lambda_m \approx 2.5$. In Fig. 2, the time dependence of a typical cross section through one of the particles is illustrated. During dissolution, the volume fraction at the center of the particle reduces to $\phi_B \sim 0.7$, and the interface between the phases broadens. After quenching, the size of the core does not change significantly, although its concentration does; first ϕ_B decreases to a minimum of ~ 0.25 at $\tau/\Delta\tau = 6000$, before starting to increase. Coarsening of the core is prevented by the surrounding shell; it is more favorable for polymers within the core to diffuse through the shell into the surrounding matrix. Eventually the core disappears and the particles become uniformly rich in component B. The dynamics of the process, as well as the effect of varying the time at which the quench is applied on the core-shell structure, is further explored in Fig. 3. In each case, the core develops after ≈ 200 time steps, indicative of the time required for a structure to develop from the random fluctuations, and the core-shell structure becomes most prominent after $\approx$ 1000–2000 time steps. In the inset, the maximum difference between ϕ_B in the core and shell, that occurs during the quench, is shown for three different initial particle sizes, as a function of quench time. For $R = 16$ a quench applied at $\tau/\Delta\tau \approx 6000$ results in the possibility of the most distinct structures. If the quench is too soon, i.e., $\tau/\Delta\tau \lesssim 1000$, after dissolution has started, the particles will simply act as nucleation sites for the phase separation; no significant core develops. If too much dissolution is allowed, i.e., $\tau/\Delta\tau \approx 16\,000$, then phase separation will proceed as if from a homogenous blend. If the particle is too small, e.g., $R = 12$, compared to λ_m, the core-shell structure will not be too well developed. On the other hand, for $R = 20$, it is clear that a large range of quench times will result in a well defined core-shell morphology.

Particles with a greater radius than $R = 20$ develop more complex structures, as illustrated in Fig. 4, for 20 particles rich in component B, each of radius 32 lattice steps. The grid size is 512^2, so that the volume fraction of B is $\phi_B \approx 0.27$. Δx, $\Delta\tau$, and N were the same as in the previous simulation. The spinodal boundary is now $\chi_s = 0.0125$, and we choose $|\chi - \chi s| = 0.000\,26$. Because of the larger size of the particles the quench was applied when $\tau/\Delta\tau = 20\,000$. The larger particle size corresponds to $2R/\lambda_m \approx 5$, enabling concentric rings of concentration to evolve. The snapshots suggest that there exists a central core rich in A, surrounded by three rings,

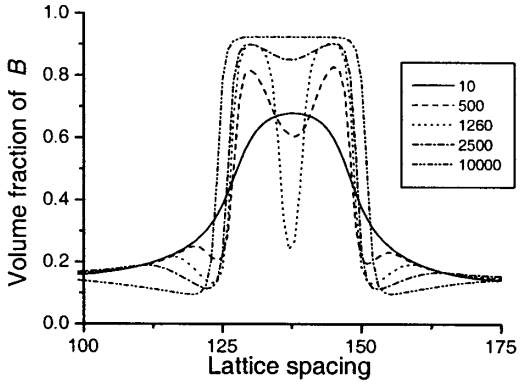

FIG. 2. Typical time evolution of the one-dimensional cross section through one of the particles ($R = 16$). Numbers in the legend refer to time steps, $\tau/\Delta\tau$, after the quench.

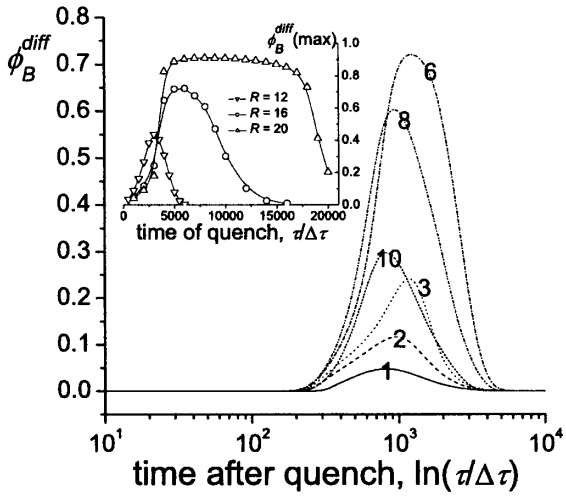

FIG. 3. The difference, $\phi_B^{\rm diff}$, between the maximum value of ϕ_B in the shell and the minimum value of ϕ_B in the core, averaged over all particles ($R = 16$), as a function of time after quench, for different times at which the quench is applied. The latter is indicated by the numbers on each curve, in thousands of $\tau/\Delta\tau$. The inset shows how the maximum difference varies as a function of the time at which the quench is applied for three different initial particle sizes.

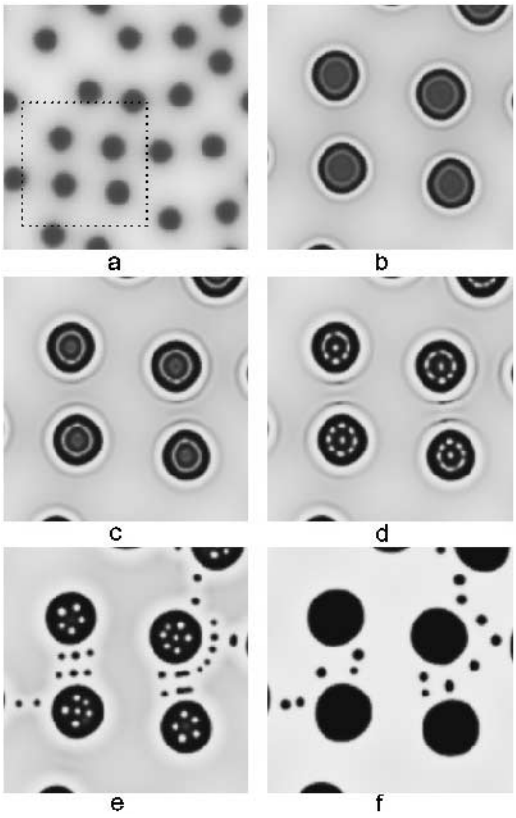

FIG. 4. Development of the morphology following the quench into the spinodal region, for 20 particles with $R = 32$. Time steps, $\tau/\Delta\tau$, following the quench: (a) 10, (b) 780, (c) 1450, (d) 2194, (e) 6188, and (f) 40 000. Only a selected 256^2 area of the simulation, corresponding to the boxed region in (a) is shown in (b) to (f).

rich in B, A, and B, respectively. The ring of component A eventually breaks up, leaving several small droplets within the particles, roughly equidistant from the center. Again, coarsening eventually leads to homogenous particles.

In summary, we have modeled a two-stage dissolution-quench process. Unusual transient morphologies develop, which, if frozen, may lead to useful material properties. Although there are a number of parameters that can be varied for any given system, the presented results indicate that the appearance of such structures is ubiquitous. In future work we will elaborate further on the effect of changing the various parameters, including the quench depth, on the detailed nature of the process. Importantly, from a technological viewpoint, the difference between the composition of the core and the shell can be large, and we have quantifiably (at least in terms of the reduced variables) shown how, for a fixed quench depth, the core-shell structure may be maximized by varying (i) the time at which the quench is applied, and (ii) the time at which the sample is frozen and morphology development arrested. It is the former that, if suitably chosen, allows for greater control over the morphology. Significantly, the optimum time to arrest structural development does not vary noticeably with the time at which the quench is applied. We have shown that an important dimensionless parameter for targeting particular morphologies is $2R/\lambda_m$. The preferred initial length scale λ_m can be tuned experimentally by varying the quench depth. The greater the quench depth, the smaller the λ_m. Our results suggest that a guideline for producing single core-shell particles is $3.5 \gtrsim 2R/\lambda_m \gtrsim 1.5$. For particles smaller than this no core develops, whereas more complex morphologies result for larger particles.

*Electronic address: nigel.clarke@durham.ac.uk

[1] A. C. Edrington, A. M. Urbas, P. DeRege, C. X. Chen, T. M. Swager, N. Hadjichristidis, M. Xenidou, L. J. Fetters, J. D. Joannopoulas, Y. Fink, and E. Thomas, Adv. Mater. **13**, 421 (2001).
[2] J. J. M. Halls, C. A. Walsh, N. C. Greenham, E. A. Marseglia, R. H. Friend, S. C. Moratti, and A. B. Holmes, Nature (London) **376**, 498 (1995).
[3] M. Berggren, O. Inganas, G. Gustafsson, J. Rasmusson, M. R. Andersson, and T. Hjertberg, Nature (London) **372**, 444 (1994).
[4] S. Puri and H. L. Frisch, J. Phys. Condens. Matter **9**, 2109 (1997).
[5] K. Binder, J. Non-Equilib. Thermodyn. **23**, 1 (1998).
[6] M. Boltau, S. Walheim, J. Mlynek, G. Krausch, and U. Steiner, Nature (London) **391**, 877 (1998).
[7] B. D. Ermi, G. Nisato, J. F. Douglas, J. A. Rogers, and A. Karim, Phys. Rev. Lett. **81**, 3900 (1998).
[8] A. M. Higgins and R. A. L. Jones, Nature (London) **404**, 476 (2000).
[9] A. Karim, J. F. Douglas, G. Nisato, D.-W. Liu, and E. J. Amis, Macromolecules **32**, 5917 (1999).
[10] B. P. Lee, J. F. Douglas, and S. C. Glotzer, Phys. Rev. E **60**, 5812 (1999).
[11] K. D. Kwak, M. Okada, T. Chiba, and T. Nose, Macromolecules **26**, 4047 (1993).
[12] H. Tanaka, Phys. Rev. E **47**, 2946 (1993).
[13] M. Hayashi, H. Jinnai, and T. Hashimoto, J. Chem. Phys. **113**, 3414 (2000).
[14] J.W. Cahn and J. E. Hilliard, J. Chem. Phys. **28**, 258 (1958).
[15] H. E. Cook, Acta Metall. **18**, 297 (1970).
[16] P. G. deGennes, J. Chem. Phys. **72**, 4756 (1980).
[17] P. Pincus, J. Chem. Phys. **75**, 1996 (1981).
[18] K. Binder, J. Chem. Phys. **79**, 6387 (1983).
[19] S. C. Glotzer, Annu. Rev. Comput. Phys. **2**, 1 (1995).
[20] P. J. Flory, *Principles of Polymer Chemistry* (Cornell University Press, Ithaca, N.Y., 1953).